MICROSTRUCTURE AND ANISOTROPY OF CREEP IN Ti-46Al-2W-0.5Si CASTINGS

A. DLOUHÝ, K. KUCHAŘOVÁ, M. SVOBODA, R. VÁLEK AND J. BŘEZINA

Institute of Physics of Materials, Academy of Sciences of the Czech Republic, Žižkova 22, 616 62 BRNO, Czech Republic

ABSTRACT

The present study investigates microstructure and creep behaviour of the cast alloy Ti-46Al-2W-0.5Si (at-%) at temperatures 700, 750 and 800°C and applied stresses between 250-420 MPa. Solidification of the alloy during precision casting is associated with two processes: (i) the growth of the $[0001]_\alpha$ oriented columnar grains from the mould wall into the cast interior and (ii) the enrichment of the central part of the cast with aluminium. The first process results in a fully lamellar microstructure where lamellae are preferentially oriented parallel to the cast surface. The second process contributes to the development of the duplex microstructure in the central part of the cast. It is shown that distinct microstructural types in different regions of the cast result in different creep strengths. Specimens taken from inside of the cast and oriented parallel to the cast bar axis exhibited the lowest creep strength while similarly oriented specimens cut from the fully lamellar region near the cast surface were the strongest. The third type of the creep specimens cut out of the central region of the cast and oriented perpendicular to the cast bar axis showed the intermediate creep strength. The observed variations of the creep strength are associated with the preferential orientation of the lamellae and with the fraction of equiaxed γ-grains in the duplex regions of the cast.

KEYWORDS

Precision casting, γ-TiAl, creep strength, fully lamellar microstructure, duplex microstructure.

INTRODUCTION

In recent years, there has been a considerable effort directed towards a development of a creep resistant γ-TiAl based alloy which would meet strong mechanical and oxidation requirements set for long blades in the low pressure section of gas turbines. As a result, an alloy ABB-IMN2 with the chemical composition Ti-46Al-2W-0.5Si (at-%) has been patented [1]. Further research has been performed to optimise the heat treatment, microstructure and related properties of the ABB-IMN2 alloy [2]. Since the precision casting is one of the most cost effective production routes suitable for the fabrication of gas turbine components, the relation between the processing route and the final properties of the ABB-IMN2 castings has also been studied. Main issues are particularly associated with the non-homogeneous microstructure observed in different parts of the cast components. The cast microstructure is difficult, if possible at all, to break and homogenize during the subsequent heat treatment. It appears that certain degree of microstructural inhomogeneity has to be accepted as the consequence of selected processing and heat treatment paths. The present study investigates the influence of the inhomogeneous cast microstructure on the ABB-IMN2 alloy creep behaviour.

EXPERIMENTAL DETAILS

Investigated alloy and creep specimens

The ABB-IMN2 alloy cast by Howmet Research Corp. and supplied by ALSTOM Power has been studied. The alloy was cast in the form of a rectangular bar with the cross-section of 75 x 15 mm^2. The macrostructure of the bar shown in Fig. 1a consists of two columnar regions that spread from the bar surfaces into the bar interior. Grains inside of the columnar regions usually possess the lamellar microstructure. The central part of the bar in which the two columnar regions meet exhibits a duplex microstructure, Fig. 1b.

Three different types of tensile creep specimens (parallel lamellar - **PL**, parallel duplex - **PD** and transverse duplex - **TD**) were cut out of the cast bar. As it is shown in Fig. 2, the axis of

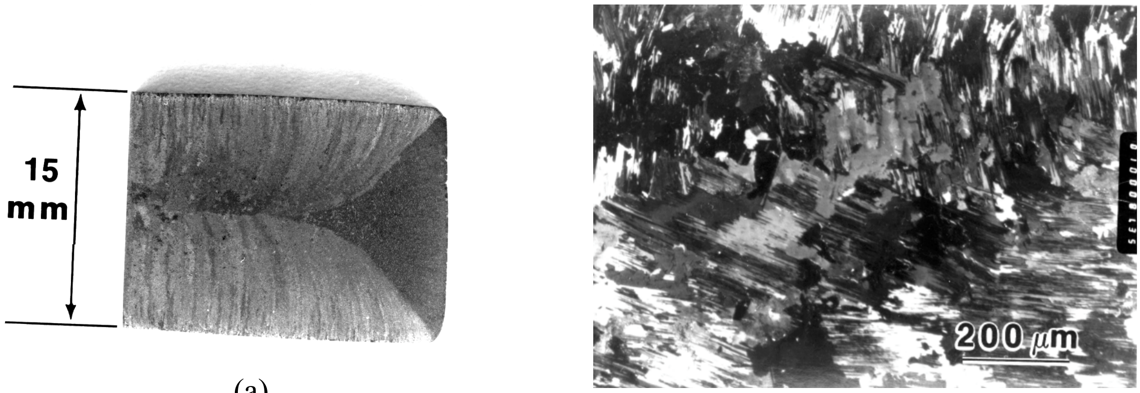

(a) (b)

Fig. 1. The as-cast macro- (a) and micro-structure (b) of the Ti-46Al-2W-0.5Si (at-%) alloy. Columnar grains in (a) are lamellar while the central part of the cast possesses a duplex microstructure shown in (b).

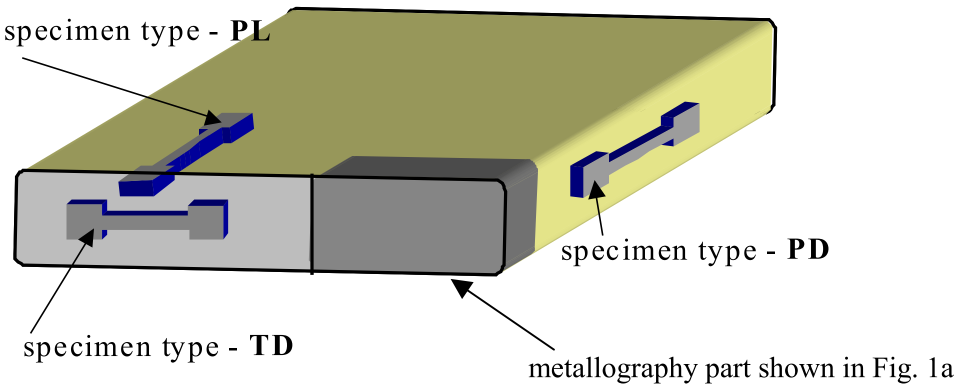

Fig. 2. Three different creep specimen orientations with respect to the cast Ti-46Al-2W-0.5Si (at-%) bar. While the gauge length part of PD and TD specimens is always cut from a central region of the cast, PL specimens are cut from regions closer to the cast surface.

PL and PD specimen types was parallel with the bar axis. The specimens PL were taken completely from the columnar region where grains are fully lamellar. On the other hand, the gauge length of specimens PD was cut entirely off the duplex material in the central area of the cast. The specimens TD were also taken from this central part of the bar, however, their tensile axis was oriented perpendicular to the bar axis.

Creep testing

Creep tests were performed in tension under the constant applied stress in purified argon atmosphere. True strain-time readings were continuously recorded by a PC-based data acquisition system. The testing temperature was maintained constant within ±1°C along the specimen gauge length and invariable during the tests. These measures yielded a good reproducibility of creep results. The three types of creep specimens (PL, PD and TD) with gauge part dimensions of 25 x 4 x 3.2 (in mm) were tested in the range of temperatures (700-800°C) and applied stresses (250-420 MPa).

Metallography methods

The microstructure of the as-cast alloy was investigated using conventional light microscopy - LM (NEOPHOT 32, ZEISS – microscope), scanning electron microscopy – SEM (PHILIPS SEM 505 – microscope) and transmission electron microscopy – TEM (PHILIPS CM12 TEM/STEM – microscope equipped with the Ultra-Thin window EDAX Phoenix analyzer). Sixteen back scattered electron SEM images (BSE) were taken from the metallographic cross-section shown in Fig. 1a. The image area 600 x 400 μm^2 sampled the cross-section area from the top edge to the bottom edge with the sampling step of 1 mm. Two of these SEM micrographs are presented in Fig. 3 that correspond to the last sampling step (Fig. 3a, where the bottom edge of the cast is clearly seen) and to the seventh sampling step (Fig. 3b, where the central part of the cast is documented). The interdendritic regions in Fig. 3b are Al rich and thus they give rise to a good contrast in BSE mode since they appear darker than the surrounding Ti-rich dendritic material.

Two characteristics of the as-cast microstructure were quantitatively assessed from the SEM

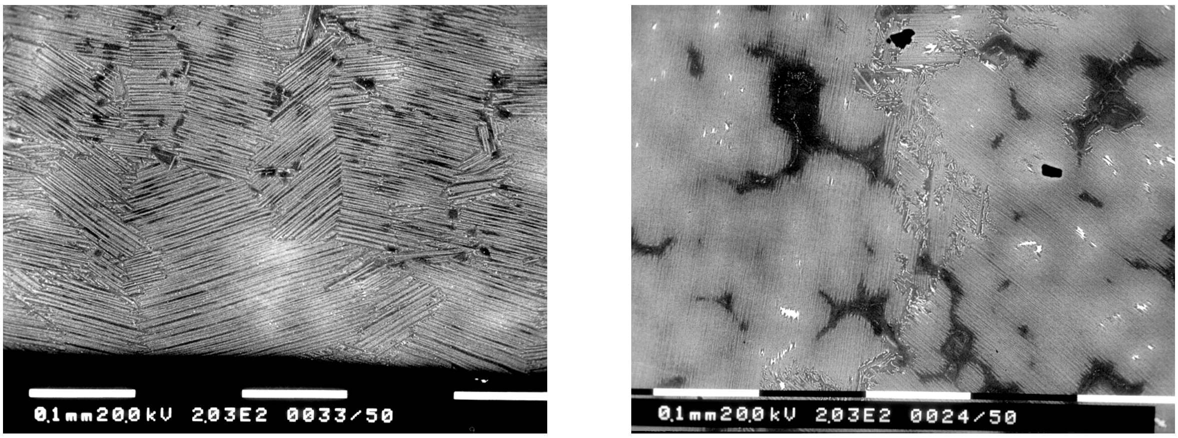

(a) (b)

Fig. 3. SEM micrographs obtained in BSE mode. (a) the lamellar grains close to the cast surface, (b) the dendritic lamellar and interdendritic γ regions inside the cast, 6 mm from the cast surface.

micrographs using a PC-based DIPS image analysis system: (i) the angle included between lamellae of each lamellar grain and the bottom or top surface edges of the cast and (ii) the fraction of interdendritic regions in the micrograph area. The quantification of the as-cast microstructure aimed, first, at establishing the relationship between the grain area and the inclination of the lamellae in the particular grain and, second, at the dependence showing how the fraction of interdendritic regions changes with the distance from the cast surface.

A special care was also given to the preparation of TEM foils to avoid any damage due to thinning operations. Slices cut out of the creep specimen gauge length were ground on emery papers to the thickness of 0.3 mm. From this point on only chemical methods were applied. The double jet TENUPOL equipment was used for final perforation of the foil. The electrolyte $HClO_4$ (5%) and methanol (95%) was kept at -50°C. Examples of TEM micrographs taken for the as-cast microstructure are presented in Figs. 4, 5 and 6.

RESULTS AND DISCUSSION

As-cast microstructure

A TEM analysis confirmed that the grains inside of the columnar regions are fully lamellar with the mean interface spacing of (450 ± 35) nm, Fig. 4. The TEM study also confirmed that the microstructure in the central part of the cast is more irregular. In this region shown in Fig. 5, the lamellar grains often coexist with the γ-grains that do not exhibit any lamellae.

The chemical composition of the alloy has been studied in the STEM mode. The composition of the matrix phase corresponds - within the accuracy of the measurement - to the nominal composition stated by the alloy producer. In addition to the matrix phase, two other secondary phases can clearly be distinguished. The first type of precipitates is enriched with W and this phase is further referred to as the W-rich phase. The particles of the other type contain only limited amount of tungsten and their composition can be approximately described as Ti_3AlSi. These precipitates are further referred to as Si-rich phase. The two types of secondary particles differ not only in the chemical composition but their morphology and space distribution are also different. While the elongated W-rich particles are almost exclusively

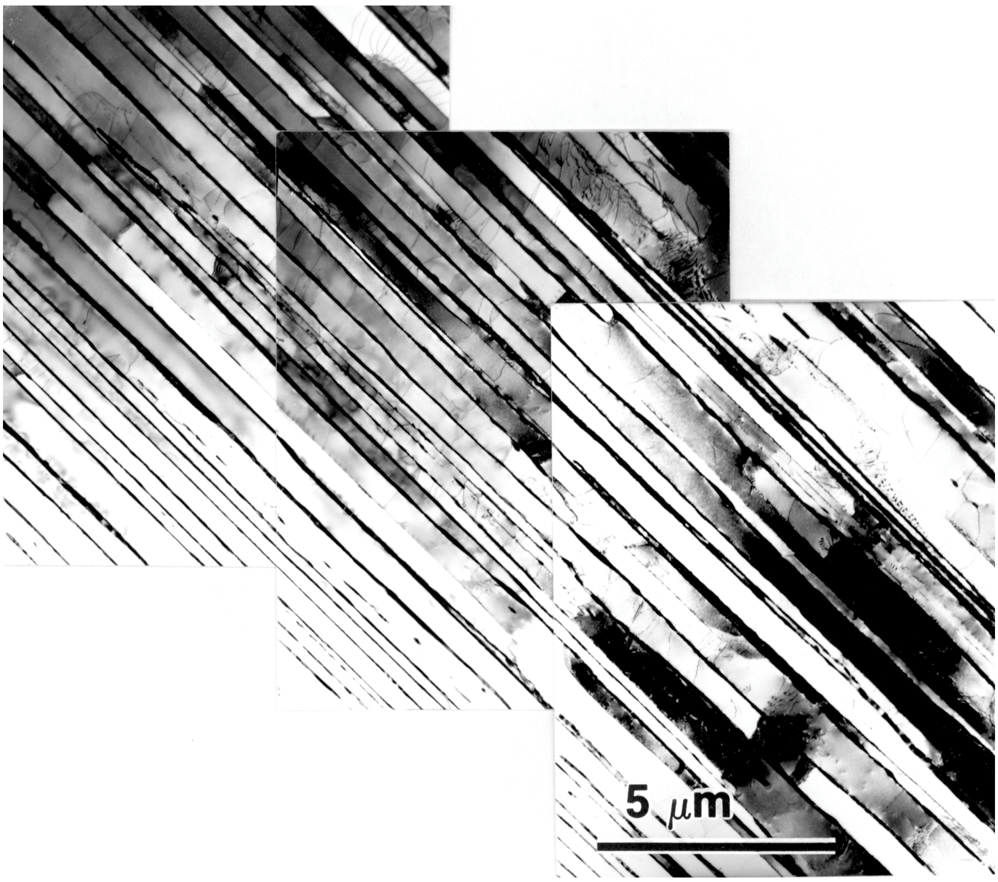

Fig. 4. TEM micrograph shows the lamellar structure of the Ti-46Al-2W-0.5Si (at-%) alloy inside the grain situated in the columnar region of the cast bar. The mean lamellar spacing (interface to interface) was estimated as 450 ± 35 nm.

situated in the lamellar boundaries (particle P2 in Fig. 6a) the globular Si-rich particles precipitate inside the matrix and are not associated with the lamellae (particle P3 in Fig. 6b). The space distribution of these Si-rich particles is often uneven, they frequently form larger groups as it is documented in the lower left corner of Fig. 5.

The relation between the grain area and the angle that lamellae of the grain include with traces of the top or bottom surface of the cast was found in three steps. In the first step, the area of lamellar grains and their centre of gravity were obtained. In the second step, the DIPS system evaluated the angle between the cast surface and direction lines, which approximated the inclination of lamellae in each lamellar grain. The centre of gravity of each direction line was also found. In the third step, the spacing between the centre of gravity of *one particular grain* and the centre of gravity of all direction lines in the micrograph was computed. In this way, a set of spacings was obtained for each individual grain. The minimum spacing of the set indicated that the corresponding direction line characterizes the orientation of lamellae in *the particular grain*. Therefore the relationship between the grain area and the orientation of lamellae in this grain can be established on the basis of minimal spacing between centres of gravity of the grain and its corresponding direction line.

Results of the quantitative image analysis are presented in Fig. 7, where the first plot (Fig.7a) clearly shows that the fraction of the interdendritic regions increases with increasing distance from the surface of the cast bar. These interdendritic regions are Al-rich and they solidify directly as pure γ-grains without any subsequent $\alpha \rightarrow \gamma$ transformation which would give rise to the lamellar microstructure [3]. The fraction of these γ-grains can be as high as 50% in the central part of the cast bar.

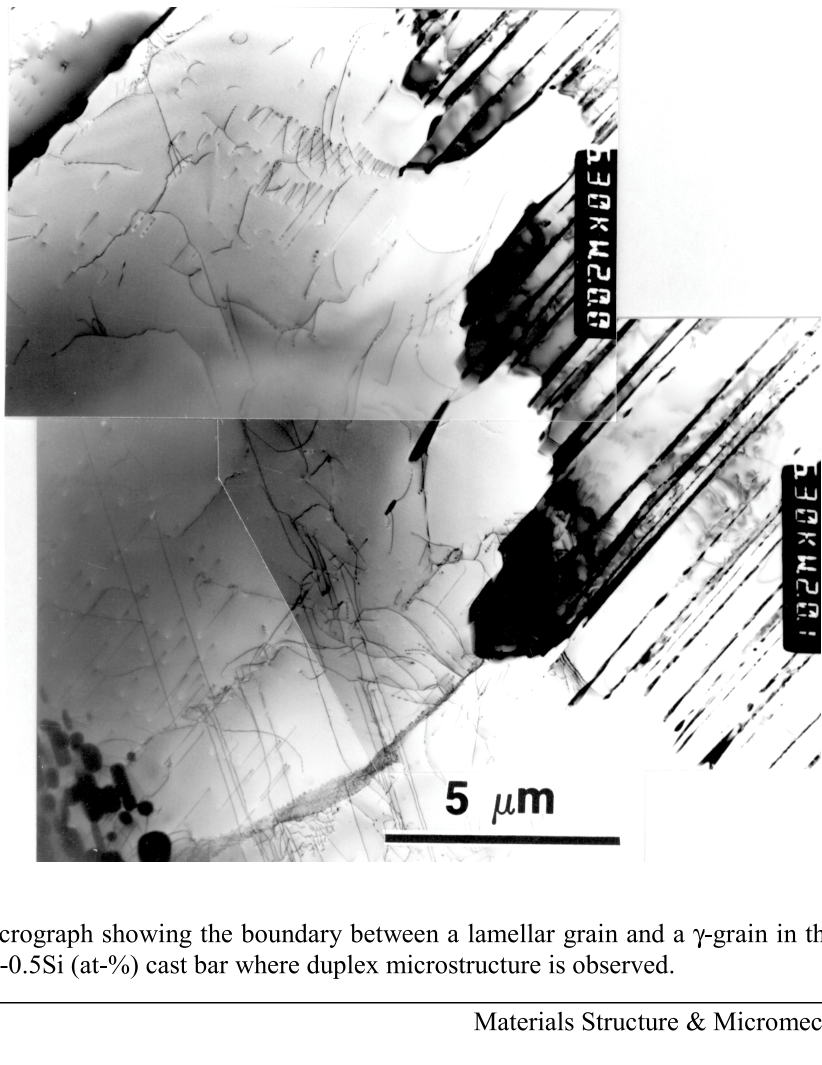

Fig. 5. TEM micrograph showing the boundary between a lamellar grain and a γ-grain in the central part of the Ti-46Al-2W-0.5Si (at-%) cast bar where duplex microstructure is observed.

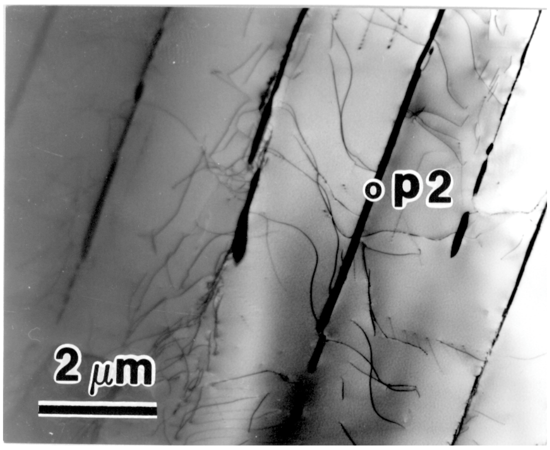

(a)

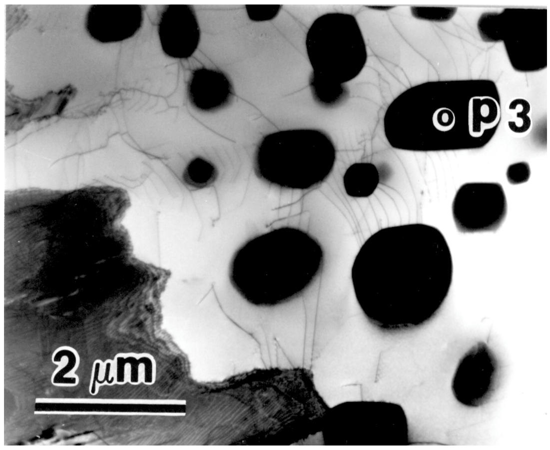

(b)

Fig. 6. TEM micrographs showing the distribution of W-rich (Fig. 6a) and Si-rich (Fig. 6b) phases in the as-cast microstructure of the Ti-46Al-2W-0.5Si (at-%) alloy. W-rich particles like P2 are always associated with lamellar boundaries, while Si-rich particles like the particle P3 can be found inside γ-grains where they form larger conglomerates.

Figure 7b presents the distribution of the angle between lamellae and surface traces in the metallographic cross-section of Fig. 1a. The distribution indicates that the lamellae in the large majority of grains (large part of the evaluated area of the cross-section) are almost parallel to the top or bottom cast surfaces (the angles, which these lamellae include with the surface traces fall in the angular range (–20°,+20°)). However, lamellae in many lamellar grains situated close to the centre of the cast bar were oriented differently. These grains thus contributed to the side maxima presented in the plot of Fig. 7b.

Creep

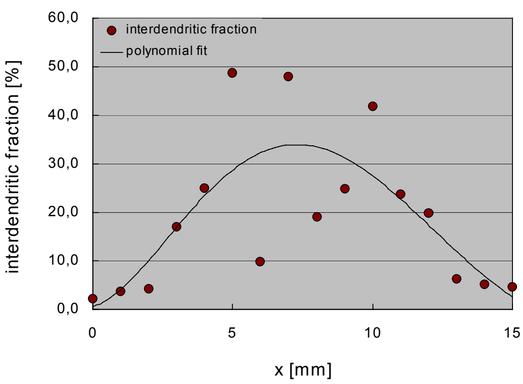

(a)

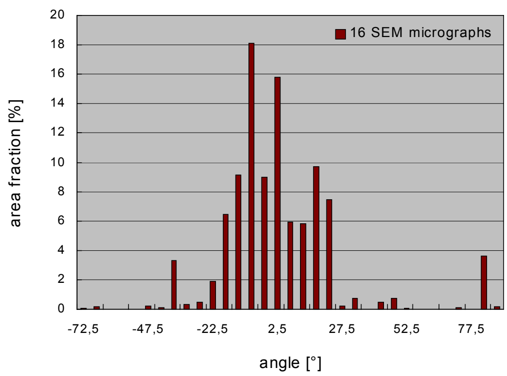

(b)

Fig. 7. (a) Fraction of interdendritic regions in the Ti-46Al-2W-0.5Si (at-%) cast increases with distance from the cast surface, the x-coordinates 0 and 15 mm correspond to the top and bottom surface, respectively. (b) Distribution of the angle included by lamellae and surface traces in the cross-section of Fig. 1a.

Creep curves recorded at 750°C and 350 MPa are presented in Fig. 8a. These creep curves strongly suggest that different types of tensile creep specimens (PL, PD and TD, see Fig. 2) behave differently at the same external conditions. The PD specimen exhibits the lowest creep strength (the highest creep rate), creep strength of the TD specimen is intermediate and the PL specimen possesses the best creep strength. As can be seen in Fig. 8a, there is nearly an order of magnitude difference between the weakest and the strongest variant in terms of creep rate and thus this difference should be considered as relevant. The question certainly arises whether the difference observed at 750°C and 350 MPa is just due to some random variations of microstructure or whether it results systematically due to the fact that particular specimen types were cut out of different parts of the cast bar which exhibited systematically different microstructures reported in the previous section. The answer is given in the plot of Fig. 8b which shows the dependence of the minimum creep rate on the applied stress. It can be clearly seen that the observed creep strength variations associated with PD, TD and PL specimen types show the same trend not only when the tests are performed under different applied stress (400 MPa at 750°C), but also when both, the testing temperature and applied stress are changed to 800°C and 300 MPa, respectively. These results strongly suggest that the observed creep strength differences are systematic and reproducible and that they are associated with different microstructural types presented in the original cast bar.

It should be highlighted that the creep strength differences observed for the PD and PL type specimens are in agreement with some earlier results obtained for similar materials [4]. According to the quantitative microstructural investigation performed in this study (Fig. 7a), the PD and TD specimens were taken from the central part of the cast bar with duplex type of microstructure, while the PL specimens were cut from nearly lamellar regions. Therefore, the creep strength variations associated with PD and PL specimens are also in line with the generally accepted view that the duplex microstructure possesses lower creep strength as compared to the fully lamellar one [5].

On the other hand, smaller but systematic differences in creep strength between PD and TD specimens are rather unexpected and require further investigation. A tentative explanation could be based on the fact that lamellae in lamellar grains, which are situated in the central part of the cast, are frequently perpendicular to the top and bottom surfaces of the cast bar (see side maxima in Fig. 7b). Assuming that these lamellae are also perpendicular to the axis of TD specimens and parallel to the axis of PD specimen, the associated creep strength variations would be in agreement with the reported dependence of strength on the orientation of polysynthetically twinned (PST) crystals [6,7]. However, the above assumption concerning the orientation of lamellae with respect to the PD and TD specimen axes should first be verified by means of the back scattered electron diffraction (EBSP method [8]) before more definite conclusion could be drawn. In passing we note, that the EBSP technique is not available to the authors at present.

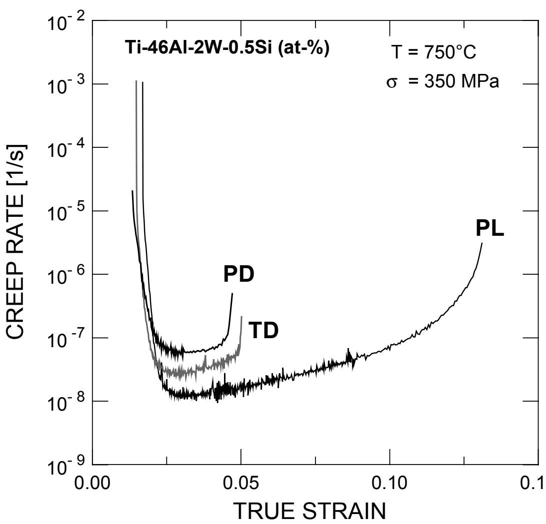

(a)

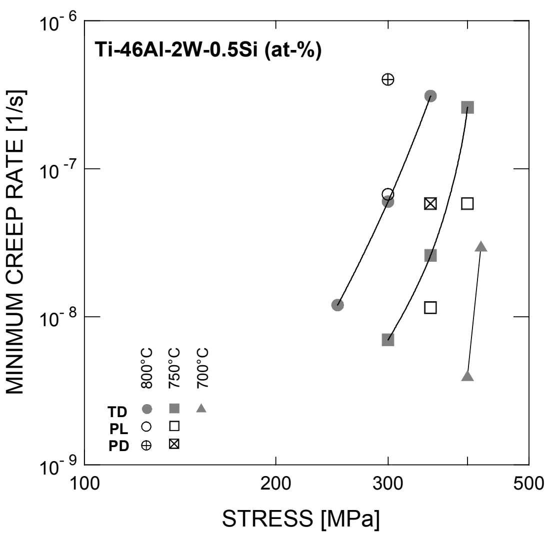

(b)

Fig. 8. (a) Creep curves of three different types of specimens (PL, PD and TD, see Fig. 2) obtained at 750°C and 350 MPa. (b) Dependence of minimum creep rate on the applied stress for all the three specimen types and different temperatures.

SUMMARY AND CONCLUSIONS

The microstructure and creep properties of the cast Ti-46Al-2W-0.5Si (at-%) alloy were investigated in the present study. The results support following conclusions.

1) Two columnar regions that meet in the middle of the casts are observed in the cast bar. The grains inside of the columnar regions possess lamellar structure with the mean interface spacing of (450 ± 35) nm. In the middle of the casts more irregular duplex microstructure has been found.

2) The local composition analysis by EDAX provided evidence that, along with the matrix phase there are two distinct types of secondary particles. Elongated W-rich precipitates, which are always situated in the lamellar boundaries and the Si-rich globular precipitates, which are fully embedded in the matrix with no apparent connection to the lamellae.

3) A considerable anisotropy of creep in the cast material has been found. The specimens taken out of the fully lamellar region with the tensile axis parallel to the cast rod axis exhibited the highest creep strength in the temperature range 750-800°C and for applied stresses between 300-400 MPa.

ACKNOWLEDGEMENT

The experimental alloy has been provided by Dr. M. Nazmy (ALSTOM Power, Baden). Financial supports from the Ministry of Education, Youth and Sports of the Czech Republic (contract no. COST 522.100) and from AS CR (contract no. S2041001) are acknowledged.

REFERENCES

[1] Nazmy M. and Staubli M.: U.S. Pat. no. 5,207,982 and European Pat. no. 4555005 B1.

[2] Nazmy M. and Lupinc V.: In: *Materials for Advanced Power Engineering 1998, Part II, Proceedings of the Sixth Liège Conference*, J. Lecomte-Beckers et al. (Eds.). Forschungszentrum Jülich, Jülich, 1998, pp. 933-944.

[3] Naka S.: In: *Materials for Advanced Power Engineering 1998, Part II, Proceedings of the Sixth Liège Conference*, J. Lecomte-Beckers et al. (Eds.). Forschungszentrum Jülich, Jülich, 1998, pp. 945-960.

[4] Lundström D., Knutson-Wedel M. and Karlsson B., In: *Materials for Advanced Power Engineering 1998, Part III, Proceedings of the Sixth Liège Conference*, J. Lecomte-Beckers et al. (Eds.). Forschungszentrum Jülich, Jülich, 1998, pp. 1229-1238.

[5] Appel F. and Wagner R.: *Mat. Sci. Eng.* R22, (1998) 187.

[6] Fujiwara T., Nakamura A., Hosomi M., Nishitani S. R., Shirai Y. and Yamaguchi M.: *Phil. Mag.* 61, (1990) 591.

[7] Wegmann G., Suda T. and Maruyama K.: In: *Creep and Fracture of Engineering Materials and Structures, Proceedings of the CFEMS 8*, T Sakuma and K. Yagi (Eds.). *Key Eng. Mat.* 171-174, Trans Tech Publications, Uetikon-Zuerich, 2000, pp. 709-716.

[8] Adams B. L., Wright S. I. and Kunze K.: *Metall. Trans.* A24, (1993) 819.